J Neurophysiol 102: 259–271, 2009.
First published April 22, 2009; doi:10.1152/jn.00065.2009.

Regulation of Cation Channel Voltage and Ca^{2+} Dependence by Multiple Modulators

Kate E. Gardam and Neil S. Magoski
Department of Physiology, Queen's University, Kingston, Ontario, Canada

Submitted 21 January 2009; accepted in final form 15 April 2009

Gardam KE, Magoski NS. Regulation of cation channel voltage and Ca^{2+} dependence by multiple modulators. *J Neurophysiol* 102: 259–271, 2009. First published April 22, 2009; doi:10.1152/jn.00065.2009. Ion channel regulation is key to controlling neuronal excitability. However, the extent that modulators and gating factors interact to regulate channels is less clear. For *Aplysia*, a nonselective cation channel plays an essential role in reproduction by driving an afterdischarge in the bag cell neurons to elicit egg-laying hormone secretion. We examined the regulation of cation channel voltage and Ca^{2+} dependence by protein kinase C (PKC) and inositol trisphosphate (IP_3)—two prominent afterdischarge signals. In excised, inside-out patches, the channel remained open longer and reopened more often with depolarization from −90 to +30 mV. As previously reported, PKC could closely associate with the channel and increase activity at −60 mV. We now show that, following the effects of PKC, voltage dependence was shifted to the left (essentially enhanced), particularly at more negative voltages. Conversely, the voltage dependence of channels lacking PKC was shifted to the right (essentially suppressed). Predictably, activity was increased at all Ca^{2+} concentrations following the effects of PKC; nevertheless, Ca^{2+} dependence was actually shifted to the right. Moreover, whereas IP_3 did not alter activity at −60 mV, it drastically shifted Ca^{2+} dependence to the right—an outcome largely reversed by PKC. With respect to the afterdischarge, these data suggest PKC initially upregulates the channel by direct gating and shifting voltage dependence to the left. Subsequently, PKC and IP_3 attenuate the channel by suppressing Ca^{2+} dependence. This ensures hormone delivery by allowing afterdischarge initiation and maintenance but also prevents interminable bursting. Similar regulatory interactions may be used by other neurons to achieve diverse outputs.

INTRODUCTION

Triggering prolonged neuronal activity with a transient input is a common means to alter motor programs or secrete neuropeptide (Beurrier et al. 1999; Bicknell and Leng 1981; Dembrow et al. 2004; Soldo et al. 2004). These changes in firing are produced by persistent voltage-dependent Na^+ and Ca^{2+} channels or nonselective cation channels (Hung and Magoski 2007; Mercer et al. 2005; Swenson and Bean 2003; Tahvildari et al. 2008). Regarding the latter, cation channels are often Ca^{2+} activated, may be voltage dependent, and provide inward current by passing Na^+, K^+, and occasionally Ca^{2+} (Kononenko et al. 2004; Liman 2003; Liu et al. 2007; Obukhov and Nowycky 2005; Partridge and Swandulla 1988; Strubing et al. 2001; Swandulla and Lux 1985; Yellen 1982).

Cation channels may be regulated by phosphorylation and second messengers; for example, protein kinase C (PKC) increases the Ca^{2+} sensitivity of transient receptor potential melastatin (TRPM4) channels (Nilius et al. 2005), whereas inositol 1,4,5-trisphosphate (IP_3) directly gates olfactory neuron cation channels (Fadool and Ache 1992). Although this has the potential to evoke spiking, how multiphasic patterns of output with different firing frequencies are achieved is less apparent. One possibility would be a dynamic system of second messengers and enzymes that continually modulates a cation channel to change the depolarizing current over time.

The bag cell neurons of *Aplysia californica* initiate reproduction through an afterdischarge driven by a cation channel (Conn and Kaczmarek 1989; Kupfermann 1967, 1970; Wilson et al. 1996). Following a brief synaptic stimulus, these neurons depolarize and fire a fast (1–2 min, 4–6 Hz) and then slow (~30 min, 1–2 Hz) phase of action potentials (Kaczmarek et al. 1982). Egg-laying hormone is released during the slow phase, triggering egg deposition (Arch 1972; Loechner et al. 1990; Michel and Wayne 2002; Rothman et al. 1983). To prevent disruption of on-going reproductive behaviors, the neurons enter a lengthy refractory period where a second burst cannot be evoked (Kaczmarek et al. 1978; Kupfermann and Kandel 1970). Blocking the cation channel or interfering with channel gating factors prevents depolarization and/or afterdischarge generation (DeRiemer et al. 1985; Kachoei et al. 2006; Magoski et al. 2002; Wilson et al. 1996).

The bag cell neuron cation channel is voltage dependent and Ca^{2+} activated (Wilson et al. 1996). A close interaction with calmodulin appears to mediate Ca^{2+} dependence (Lupinsky and Magoski 2006). The channel is also modulated by closely associated kinases and phosphatases (Magoski 2004; Wilson and Kaczmarek 1993; Wilson et al. 1998). In particular, as assayed using inside-out patches, PKC can be linked to the channel and serves to increase activity (Magoski and Kaczmarek 2005; Magoski et al. 2002). During the afterdischarge, PKC is upregulated and IP_3 is elevated (Fink et al. 1988; Wayne et al. 1999); however, it is unknown whether either factor influences voltage or Ca^{2+} dependence. We now show that, whereas PKC enhances voltage dependence, it actually suppresses Ca^{2+} dependence. Also, IP_3 strongly inhibits Ca^{2+} dependence, but remarkably, PKC counteracts much of this effect. Thus rather than simply enhancing gating, cation channel regulation is multifaceted, allowing precise manipulation of activity. This would drive fast bursting but permit transition to slower spiking and eventually afterdischarge cessation. Similar mechanisms may be used by a diversity of neurons to strictly control periods of firing.

METHODS

Animals and cell culture

Adult *Aplysia californica* weighing 150–300 g were obtained from Marinus (Long Beach, CA). Animals were housed in an ~300-l

Address for reprint requests and other correspondence: N. S. Magoski, Queen's University, Dept. of Physiology, 4th Floor, Botterell Hall, 18 Stuart St., Kingston, ON K7L 3N6, Canada (E-mail: magoski@queensu.ca).

aquarium containing continuously circulating, aerated sea water (Instant Ocean; Aquarium Systems, Mentor, OH or Kent sea salt; Kent Marine, Acworth, GA) at 14–16°C on a 12:12-h light:dark cycle and fed Romaine lettuce five times a week. A few animals were housed at 18–20°C. All protocols were approved by the Queen's University animal care committee.

For primary cultures of isolated bag cell neurons, animals were anesthetized by an injection of isotonic $MgCl_2$ (50% of body weight), and the abdominal ganglion was removed and treated (for 18 h at 20–22°C) with neutral protease (13.33 mg/ml; 165859, Roche Diagnostics, Indianapolis, IN) dissolved in tissue culture artificial sea water (tcASW; composition in mM: 460 NaCl, 10.4 KCl, 11 $CaCl_2$, 55 $MgCl_2$, 15 HEPES, 1 mg/ml glucose, 100 U/ml penicillin, and 0.1 mg/ml streptomycin, pH 7.8 with NaOH). The ganglion was transferred to fresh tcASW for 1 h, after which time the bag cell neuron clusters were dissected from their surrounding connective tissue. Using a fire-polished Pasteur pipette and gentle trituration, neurons were dispersed in tcASW onto 35 × 10-mm polystyrene tissue culture dishes (Corning, Corning, NY). Cultures were maintained in tcASW in a 14°C incubator and used within 1–3 days. Salts were obtained from Fisher Scientific (Ottawa, Canada), ICN (Aurora, OH), or Sigma-Aldrich (St Louis, MO).

Excised, patch-clamp recording

Single cation channel current was measured using an EPC-8 amplifier (HEKA Electronics, Mahone Bay, Canada) and the excised, inside-out patch-clamp method. Holding potentials were applied to the patch as inverted voltages to achieve the same membrane potentials as what the channel would experience in the neuron (Penner 1995). Microelectrodes were pulled from 1.5-mm-ID, borosilicate glass capillaries (TW 150 F-4, World Precision Instruments, Sarasota, FL) and fire polished to a resistance of 2–5 MΩ when filled with normal artificial sea water (nASW; composition as per tcASW but lacking glucose, penicillin, and streptomycin) plus 20 mM tetraethyl ammonium (TEA). The TEA was added to reduce outward currents, likely through Ca^{2+}-activated K^+ channels, which interfered with resolving cation channel inward current at depolarized potentials. To lower the root mean squared noise of the current, microelectrode capacitance was reduced by coating the shank and half of the shoulder with dental wax (Heraeus Kulzer, South Bend, IN) under a dissecting microscope. Following excision, the cytoplasmic face was bathed with artificial intracellular saline (composition in mM: 500 K-aspartate, 70 KCl, 1.2 $MgCl_2$, 10 HEPES, 11 glucose, 5 EGTA, and 10 reduced glutathione, pH 7.3 with KOH). In experiments examining voltage dependence of the channel, $CaCl_2$ was added for a free Ca^{2+} concentration of 10 μM. The experiments examining Ca^{2+} dependence were performed using intracellular saline with Ca^{2+} concentrations ranging from 300 nM to 300 μM. In all cases, the added and free Ca^{2+} concentration was calculated using WebMaxC (http://www.stanford.edu/~cpatton/webmaxc/webmaxcE.htm). Current was low-pass filtered at 1 kHz using the EPC-8 Bessel filter and acquired at a sampling rate of 10 kHz using an IBM-compatible personal computer, a Digidata 1322 A/D converter (Axon Instruments, Union City, CA), and the Clampex acquisition program of pCLAMP (version 8.0, Axon Instruments). Data were gathered at room temperature (~22°C).

Patch perfusion array, drug application, and reagents

A multibarrel perfusion array was constructed by tightly aligning borosilicate square tubing (OD: 0.75 mm, ID: 0.5 mm; #8250, Vitro-Com, Mountain Lakes, NJ) attached to one another using superglue. The section of the array that was submerged into the bath did not come in contact with the superglue. The barrels at the opposite end of the array were fitted with silicone tubing (OD: 3.3 mm, ID: 0.8 mm; Cole Parmer, Vernon Hills, IL). Each of these perfusion lines was connected to a 5-ml syringe. Gravity-driven flow was controlled by an alligator clip over the tubing and setting the level of the syringes to a fixed height. When the clip was released, the result was a flow of ~1 ml/min. Any greater flow disturbed the patch and led to mechanical-based noise or seal failure. The perfusion system allowed patches to be moved from the mouth of one barrel to the next, permitting an almost instantaneous change in solutions at the face of the channel. During perfusion, the culture dish was gently drained as required using a plastic Pasteur pipette.

Drugs were made up as concentrated stock solutions and frozen at −20°C. They were introduced to the patch at the indicated working concentration, either with the perfusion array or by pipetting a small volume of stock into the culture dish. In the latter case, care was taken to pipette the stock near the side of the dish and as far away as possible from the patch at the tip of the microelectrode.

Experiments examining the effects of nucleotides or phosphorylation on voltage dependence were performed by adding a 100 mM stock solution (in water) of ATP (#A3377, Sigma-Aldrich) or adenosine 5′-(β,γ-imido)trisphosphate (AMP-PNP; #A2647, Sigma) to the bath or perfusate for a final concentration of 1 mM. A 20 mM stock solution (in water) of GTP (#G8877, Sigma) was added for final concentration of 100 μM. A final concentration of 5 mM ATP was applied at the end of experiments using AMP-PNP to ensure that AMP-PNP was not acting as a phosphate donor. Magoski and Kaczmarek (2005) showed that an increase in P_o of >25% indicated the presence of channel-associated PKC. This same criterion was used in this study.

Experiments examining the effects of IP_3 on Ca^{2+} dependence were performed using D-myo-inositol 1,4,5-trisphosphate (#I7012, Sigma), which was dissolved in water for a stock of 5 mM. This was dilulted into the perfusate at a final concentration of 5 μM.

Data analysis

To determine channel open probability (P_o), events lists were made from data files using the half-amplitude threshold criterion (Colquhoun and Sigworth 1995) of the Fetchan analysis program of pCLAMP. Fetchan was also used to generate all-points histograms for determining channel amplitude. Before analysis, data gathered at +30, 0, −15, −30, −60, and −90 mV were refiltered, using the Fetchan digital Gaussian filter, to 100, 150, 200, 250, 250, and 500 Hz, respectively. The Pstat analysis program of pCLAMP was used to read events lists and determine P_o, either automatically or manually, using the formula

$$P_o = (1 \times t_1 + 2 \times t_2 + \ldots n \times t_n)/(N \times t_{tot})$$

where t = the amount of time that n channels are open, n = the number of channels in the patch, and t_{tot} = the time interval over which P_o is measured. The number of channels in the patch was determined by counting the number of unitary current levels, particularly at more depolarized potentials (typically −15 mV). For patches containing only one channel, two open- and three closed-state time constants were determined in Pstat, by fitting probability density functions to the logarithmic distribution of event dwell times using the minimum likelihood estimation method and a simplex search. Pstat was also used to determine the mean open- and closed-state current level by fitting all-points histograms with Gaussian functions using the least-squares method and a simplex search. Channel current amplitude was calculated by subtracting the mean closed current level from the mean open current level at a given voltage.

Concentration-response curves were constructed by dividing the P_o at each Ca^{2+} concentration by the P_o at 300 μM Ca^{2+}, this normalized data was then averaged across separate patches and plotted vs. Ca^{2+} concentration using Origin (version 7, OriginLab Corporation; Northampton, MA). Curves were fit with a Hill function to yield the EC_{50} and Hill coefficient. To make P_o versus voltage relationships, P_o was normalized to P_o at +30 mV and plotted against patch holding

potential using Origin. This relationship was fit with a Boltzmann function to derive the half-maximal voltage ($V_{1/2}$) and the slope factor (k), which is the change in voltage required to move P_o e-fold. Channel current versus voltage (*I/V*) relationships were produced in Origin by plotting channel-current amplitude against patch-holding potential, and single-channel conductance was then determined by linear regression.

Data are presented as the mean ± SE. Statistics were performed using Instat (version 3.0, GraphPad Software, San Diego, CA). The Kolmogorov-Smirnov method was used to test data sets for normality. To compare multiple means, a standard one-way ANOVA with Student-Newman-Keuls post hoc test was used. Data were considered significant if the two-tailed P value was <0.05.

RESULTS

Bag cell neuron cation channel is voltage dependent

Cation channel–containing patches were excised from cultured bag cell neurons, the cytoplasmic face was exposed to the bath solution (artificial intracellular saline), and the extracellular face to the pipette solution (nASW with 20 mM TEA). The channel was readily identified as an ~2-pA inward current at a holding potential of −60 mV with a P_o that increased at more positive potentials (Lupinsky and Magoski 2006; Magoski 2004; Wilson et al. 1996). To examine voltage dependence, the patch was initially held at −60 mV and the cytoplasmic face was bathed with intracellular solution containing no ATP and 10 μM free Ca^{2+}. Subsequently, the patch voltage was changed to +30, 0, −15, −30, and −90 mV. At more positive potentials, the cation channel showed higher activity, as seen by an increasing number of openings (Fig. 1*A*). Plotting the normalized P_o versus patch voltage produced a single-channel activation curve (Fig. 1*B*; $n = 6$). A Boltzmann fit of this curve gave a $V_{1/2}$ of −33 mV and a k value of 15. Single-channel *I/V* relationships were derived by Gaussian fits to the peaks of all-points histograms from the current at each voltage (Fig. 1*C*). This represented the open

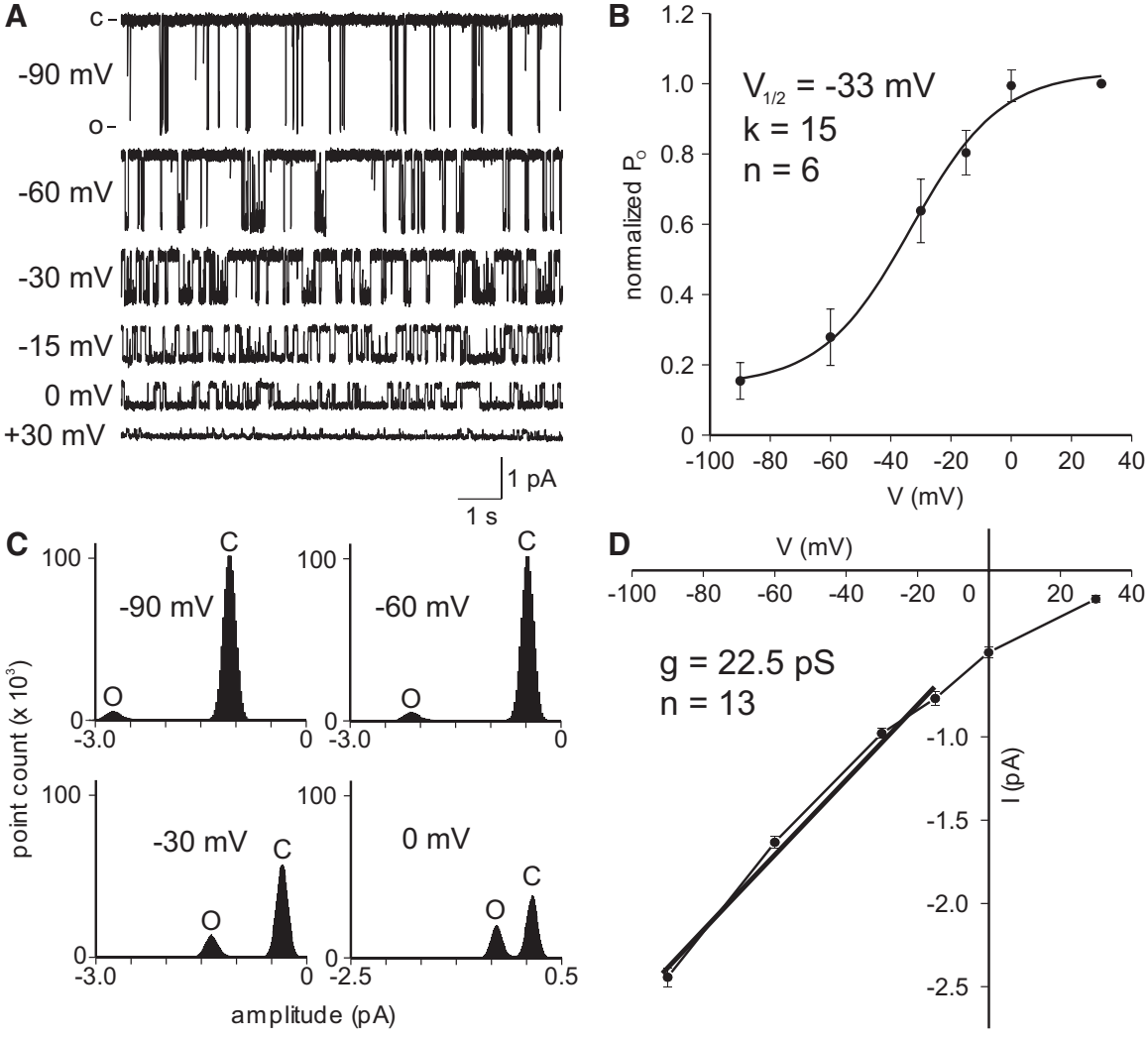

FIG. 1. The cation channel is voltage dependent. *A*: cation channel activity in an excised, inside-out patch, voltage clamped at different holding potentials. The closed state is at the top of each trace and is designated by –C, whereas the open state is at the bottom, designated by –O. As the patch is depolarized, more time is spent open (downward deflections) and less closed. *B*: voltage dependence of cation channel open probability (P_o) in 10 μM Ca^{2+} and the absence of ATP. Channel activity is normalized within each experiment to the P_o at +30 mV. *C*: the 2 peaks on each all-points histogram depict current flow during channel open (O) and closed (C) states at various voltages. Gaussian fits to these peaks are used to derive channel amplitude plotted in *D*. *D*: the single-channel *I/V* relationship shows rectification at potentials >0 mV. A conductance of 22.5 pS is derived from a linear fit of −90 to −15 mV. This represents the physiological range of the channel and avoids the region of rectification.

and closed state current. Plotting the difference between these peaks gave the *I/V* in Fig. 1*D*. Cation channel current rectified at more positive voltages; as such, only data between −90 and −15 mV were used for linear regression fit, yielding a conductance of 22.5 pS.

On occasion, cation channel recordings contained very brief (on the order of tens of milliseconds) shifts to a subconductance state. This was independent of channel modulation or gating, because these shifts occurred at most voltages and in the presence or absence of regulatory factors. The state could be recognized as a subconductance, rather than a different species of channel, because clear transitions between sub- and full-conductance were apparent (Fig. 2*A*). Were there two channels, this would require the exact, simultaneous opening of one channel and closing of the other—a very unlikely possibility. The subconductance was determined in the same manner as the full-conductance; both are plotted for comparison in Fig. 2*B*. The subconductance of the channel, based on the linear fit from −90 to −15 mV, was 13.3 pS.

Despite previous descriptions of voltage dependence, the kinetics of bag cell neuron cation channel voltage sensitivity are unknown. Ion channel kinetic states can be described by dwell time—the amount of time a channel spends in a particular closed or open state (Colquhoun and Sigworth 1995). A best-fit probability density function of the closed- and open-state histograms of true single-channel recordings, i.e., patches containing only one cation channel, gave three closed-state (τ_{C1}, τ_{C2}, τ_{C3}) and two open-state (τ_{O1}, τ_{O2}) time constants (Fig. 3, *A* and *C*). t_{C3}, the longest closed-state time constant (right-most peak on each histogram in Fig. 3*A*), shifted linearly and became shorter in duration with depolarization (Fig. 3*B*; $n = 4$). This shift represented less time spent in this closed conformation. For the open state, the longer of the two time constants, τ_{O2} (right peak on each histogram in Fig. 3*C*), became longer in duration with depolarization, thereby increasing the time spent in that state (Fig. 3*D*; $n = 5$). The other time constants did not change appreciably with voltage.

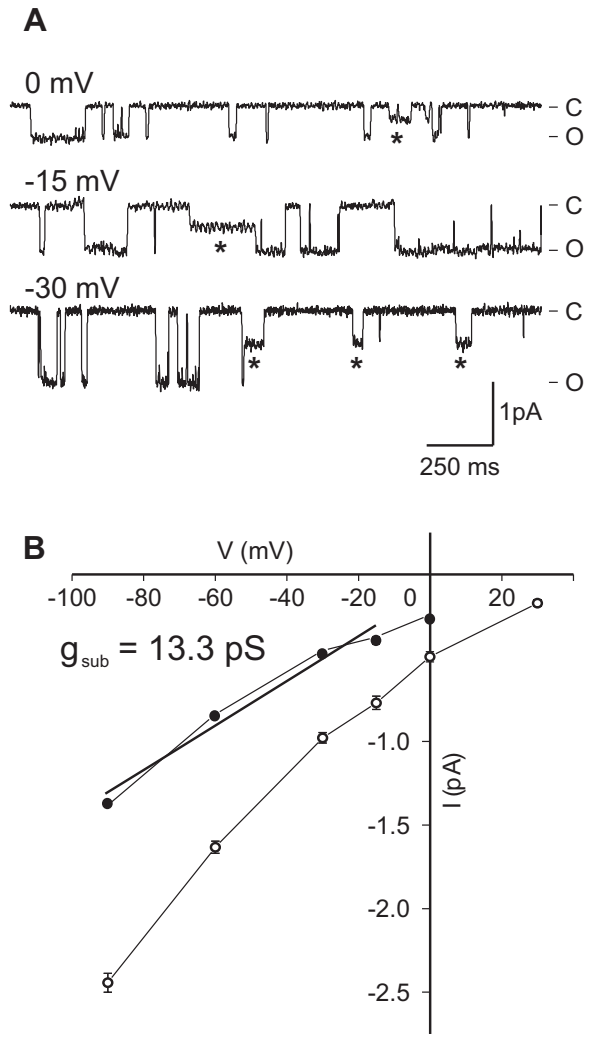

FIG. 2. A cation channel subconductance. A subconductance for the bag cell neuron cation channel is rare and occurs independent of channel kinetic or modulatory state. *A*: representative current traces of the subconductance (demarcated by *) at various voltages, showing clear transitions between sub- and full-conductance states. These are true single-channel patches. The –O refers to the full-conductance open state. *B*: single-channel *I/V* relationship of channels in the subconductance state (●) (at 0 through −90 mV, $n = 8, 9, 9, 2$, and 1, respectively; 28 patches in total) fitted between −90 and −15 mV, gives a conductance of 13.3 pS. The subconductance cannot be resolved at voltages more positive than 0 mV. The control graph (○) is replotted from Fig. 1. There was a paucity of data at the more depolarized potentials (because of resolution difficulties) and more hyperpolarized potentials (because of fewer channel openings overall).

Phosphorylation by closely associated PKC alters cation channel voltage dependence

Wilson et al. (1998) showed that PKC closely associates with the bag cell neuron cation channel and, in the presence of a phosphate source, elevates P_o. Such a phosphate source is provided by application of 1 mM ATP to the cytoplasmic face of the cation channel in excised, inside-out patches. Phosphorylation by PKC produces a characteristic, multifold increase in P_o at a holding potential of −60 mV (Magoski and Kaczmarek 2005; Magoski et al. 2002; Wilson et al. 1998). As shown by Wilson et al. (1998), this increased P_o ATP response is blocked by various PKC antagonists, indicating that it is caused by PKC-dependent phosphorylation of the channel or some nearby protein. On the contrary, a bare channel lacks known associated kinases and presents no change in P_o at −60 mV with the addition of ATP (Magoski and Kaczmarek 2005). In intact bag cell neurons, PKC is upregulated during the afterdischarge (Wayne et al. 1999), and compared with refractory

FIG. 3. The cation channel stays open longer and favors reopening with depolarization. *A*: true single-channel closed-state dwell times at 3 voltages are plotted as histograms. Each histogram is best fit with a probability density function containing 3 closed-state time constants (τ_{C1}, τ_{C2}, and τ_{C3}). The longest of these, τ_{C3}, changes with voltage, whereas the other closed time constants do not change appreciably. This is best seen in the shift of the right-most peak toward shorter durations. *B*: the length of τ_{C3} decreases linearly with depolarization—the data are normalized to −90 mV (where the τ_{C3} duration is maximal). The shortening of τ_{C3} has the effect of decreasing the amount of time the channel spends in the 3rd closed state and increasing the number of reopenings. *C*: channel open-state dwell times are also fit with a probability density function. In this case, the best fit is with 2 open-state time constants (τ_{O1} and τ_{O2}). The longer of these, τ_{O2}, also changes with voltage. This is seen in the shift of the right-most peak toward longer durations with depolarization. *D*: the length of τ_{O2} increases linearly with depolarization; the data are normalized to +30 mV (where the τ_{O2} duration is maximal). The lengthening of τ_{O2} has the effect of increasing the amount of time the channel spends in the open state.

neurons, cells that are ready to afterdischarge yield far more cation channels with associated PKC (Magoski and Kaczmarek 2005). Thus the kinase quite likely stimulates the channel during the afterdischarge; although it is unknown if any of this change in activity is achieved by regulating voltage dependence.

Cation channel voltage dependence was compared before and after addition of ATP. At an initial holding potential of −60 mV, PKC-dependent phosphorylation elevated P_o by ~250% (Fig. 4*E*). Furthermore, manipulation of the membrane potential before and after the effects of PKC showed

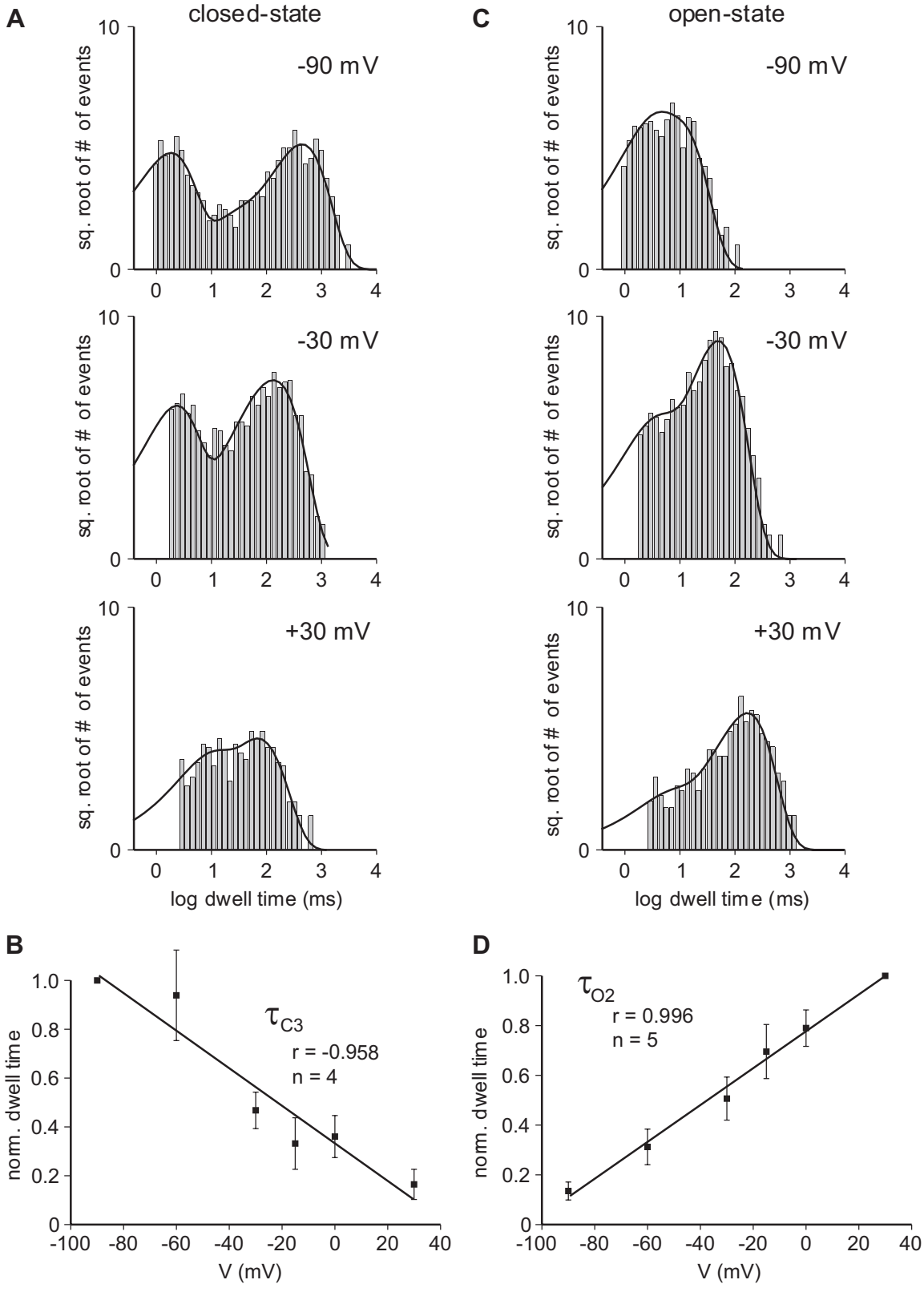

that, relative to control, the P_o was larger at all voltages in the phosphorylated state (Fig. 4*A*). Normalizing activity to the maximum P_o in these same patches showed a modest shift to the left of channel voltage dependence, with a −3-mV change in $V_{1/2}$ (Fig. 4*B*; $n = 6$). However, this difference in $V_{1/2}$ does not fully reflect the shift. The two curves, while close together at positive potentials, are far more disparate between −90 and −30 mV, i.e., the normal operating range of the channel. Following the PKC-induced P_o increase, the voltage dependence curve was essentially repositioned, with a greater amount of relative activity at more negative voltages. Thus, while the shift in $V_{1/2}$ is not large, the change in voltage dependence following PKC-dependent phosphorylation at resting potential, or during the afterdischarge, would be substantial. It is important to note that the effects of PKC were consistent for channels in neurons from a given batch of animals. Thus a better comparison of regulation is made within a group (the 2 curves on a given graph) rather than between groups (curves on different graphs).

Bare cation channels were identified as such by the application of ATP producing no appreciable change in P_o at −60 mV (Fig. 4, *C, insets*, and *E*). However, in these patches, ATP caused channel voltage dependence to shift markedly to the right, with a +14-mV change in $V_{1/2}$ (Fig. 4*C*; $n = 9$). To examine if this shift was caused by the direct effect of the nucleotide, a set of different cation channel–containing patches was exposed to AMP-PNP rather than ATP. AMP-PNP is nonhydrolysable and can act as an adenine nucleotide without serving as a phosphate donor (Yount et al. 1971). As previously reported by Wilson et al. (1998), application of 1 mM AMP-PNP had no effect on P_o at −60 mV (Figs. 4, *D, insets*, and *E*); moreover, we found that it caused a +7-mV shift in $V_{1/2}$ to the right (Fig. 4*D*; $n = 9$). To ensure that the AMP-PNP was definitely not acting as a phosphate source, the cytoplasmic face of these patches were subsequently exposed to 5 mM ATP. In three of nine patches, there was an increased P_o at −60 mV with ATP, indicating that PKC-dependent phosphorylation had not taken place in AMP-PNP alone, and the majority of patches in this set contained bare channels. Parenthetically, application of 100 μM GTP did not affect cation channel voltage dependence (data not shown) or activity (Fig. 4*E*; $n = 10$). Furthermore, as determined by linear regression of single-channel *I/V* relationships, the unitary conductance was not altered by any of the nucleotides: ATP on bare channels (21.1 vs. 21.9 pS), AMP-PNP (21.6 vs. 22.7 pS), or GTP (22.2 vs. 21.9 pS). After phosphorylation by PKC, there was a decrease in conductance (from 23.5 to 20.6 pS), although this was entirely caused by a drop in current amplitude at −90 mV.

Phosphorylation by closely associated PKC shifts cation channel Ca^{2+} dependence to the right

A potential stimulus for the cation channel is Ca^{2+} influx during the afterdischarge (Fink et al. 1988; Fisher et al. 1994; Geiger and Magoski 2008; Knox et al. 1992; Michel and Wayne 2002). Lupinsky and Magoski (2006) showed that closely associated calmodulin serves as the sensor for Ca^{2+} activation of the channel, with an EC_{50} of ~10 μM. We sought to determine whether cation channel Ca^{2+} dependence is changed following phosphorylation by associated PKC. Initially, patches were excised and perfused with artificial intracellular solution containing 30 μM free Ca^{2+} and no ATP. Ca^{2+} dependence was examined, at a holding potential of −60 mV, by first exposing the cytoplasmic face of the patch to a maximal concentration of 300 μM Ca^{2+}, followed by 30 μM, 3 μM, and 300 nM in random order. In separate experiments, the effect of PKC was observed by including 1 mM ATP in the perfusion barrels.

This study confirmed that the cation channel is Ca^{2+} dependent. Channel activity was consistently higher at greater cytoplasmic face Ca^{2+} concentrations (Fig. 5*A*; $n = 14$). The effect of Ca^{2+} was reversible and repeatable. When PKC was associated with the channel, the addition of ATP in the presence of 30 μM Ca^{2+} resulted in a 262 ± 53% increase in P_o at −60 mV (Fig. 5*C, inset*; $n = 9$). Moreover, whereas channels displaying the PKC-induced P_o increase were also clearly Ca^{2+} dependent (Fig. 5*B*), the P_o versus Ca^{2+} concentration curves showed that activity was markedly greater at every concentration compared with separate control patches not exposed to ATP (Fig. 5*C*). However, when the concentration-response curve was normalized to the activity at 300 μM, the Ca^{2+} dependence was actually shifted to the right for the PKC-associated channels (Fig. 5*D*). Specifically, the EC_{50} was 30 μM compared with 5 μM in control, with a negligible difference in the Hill coefficient (0.89 vs. 0.77).

IP_3 strongly shifts cation channel Ca^{2+} dependence to the right, and this is reversed following PKC-dependent phosphorylation

During the afterdischarge, bag cell neuron IP_3 levels are elevated and serve to liberate Ca^{2+} from intracellular stores (Fink et al. 1988). Although the higher Ca^{2+} levels may increase cation channel activity, the effects of IP_3 are also of interest. Beyond the traditional role as a Ca^{2+} release agent, IP_3 also acts on lobster neuron cation channels (Fadool and Ache 1992) and exogenously expressed TRPC3 channels (Kiselyov et al. 1998), as well as potentiates cation channel responsiveness in myocytes (Albert and Large 2003). To examine if IP_3 was a gating factor or influencing the Ca^{2+}-

FIG. 4. Phosphorylation of the cation channel by closely associated protein kinase C (PKC) shifts voltage dependence to the left. *A*: control: an excised, inside-out patch containing 3 cation channels. As the patch is depolarized from −90 through to +30 mV, there is greater channel opening. ATP: consistent with PKC-dependent phosphorylation, following application of ATP to the cytoplasmic face the P_o increases at every voltage in comparison to control. The elevation in P_o with PKC between −90 and −30 mV is readily apparent, with multilevel openings becoming far more obvious. *B*: voltage dependence of the channel is shifted to the left ($\Delta V_{1/2} = -3$ mV) in the presence of a phosphate source (1 mM ATP) when PKC is associated with the channel. The shift to the left is even more prominent in the normal operating range of the channel, i.e., between −90 and −30 mV. *C*: when the cation channel is bare, i.e., no PKC is associated, ATP shifts the voltage dependence to the right ($\Delta V_{1/2} = +14$ mV). *Insets*: ATP has no effect on P_o when the channel is bare. *D*: a nonhydrolyzable analog of ATP, adenosine 5′-(β,γ-imido)trisphosphate (AMP-PNP), shifts voltage dependence to the right ($\Delta V_{1/2} = +7$ mV), although not to the same extent as the effect of ATP on bare channels. *Insets*: AMP-PNP does not significantly change P_o from control. This data set is composed of both PKC-associated and bare cation channels. *E*: the summary data show that only phosphorylation by PKC causes a significant change in channel P_o (ANOVA, Student-Newman-Keuls post hoc test). The numbers in brackets above, below, or within each bar designate the *n* value of that data set.

dependence of the bag cell neuron cation channel, excised patches were exposed to one of three conditions: *1*) to obtain a control dose-response, 30 μM Ca^{2+} alone followed by 300 nM, 3 μM, or 300 μM Ca^{2+} in random order; *2*) to obtain a dose-response in IP_3, 30 μM Ca^{2+} alone followed by 5 μM IP_3 in 30 μM Ca^{2+} and then IP_3 in 300 nM, 3 μM, or 300 μM Ca^{2+} in random order; *3*) to test Ca^{2+} dependence after PKC-dependent phosphorylation in IP_3, 5 μM IP_3 in 30 μM Ca^{2+} followed by IP_3 in 30 μM Ca^{2+} plus 1 mM ATP and then IP_3 plus ATP in 300 nM, 3 μM, or 300 μM Ca^{2+} in random order.

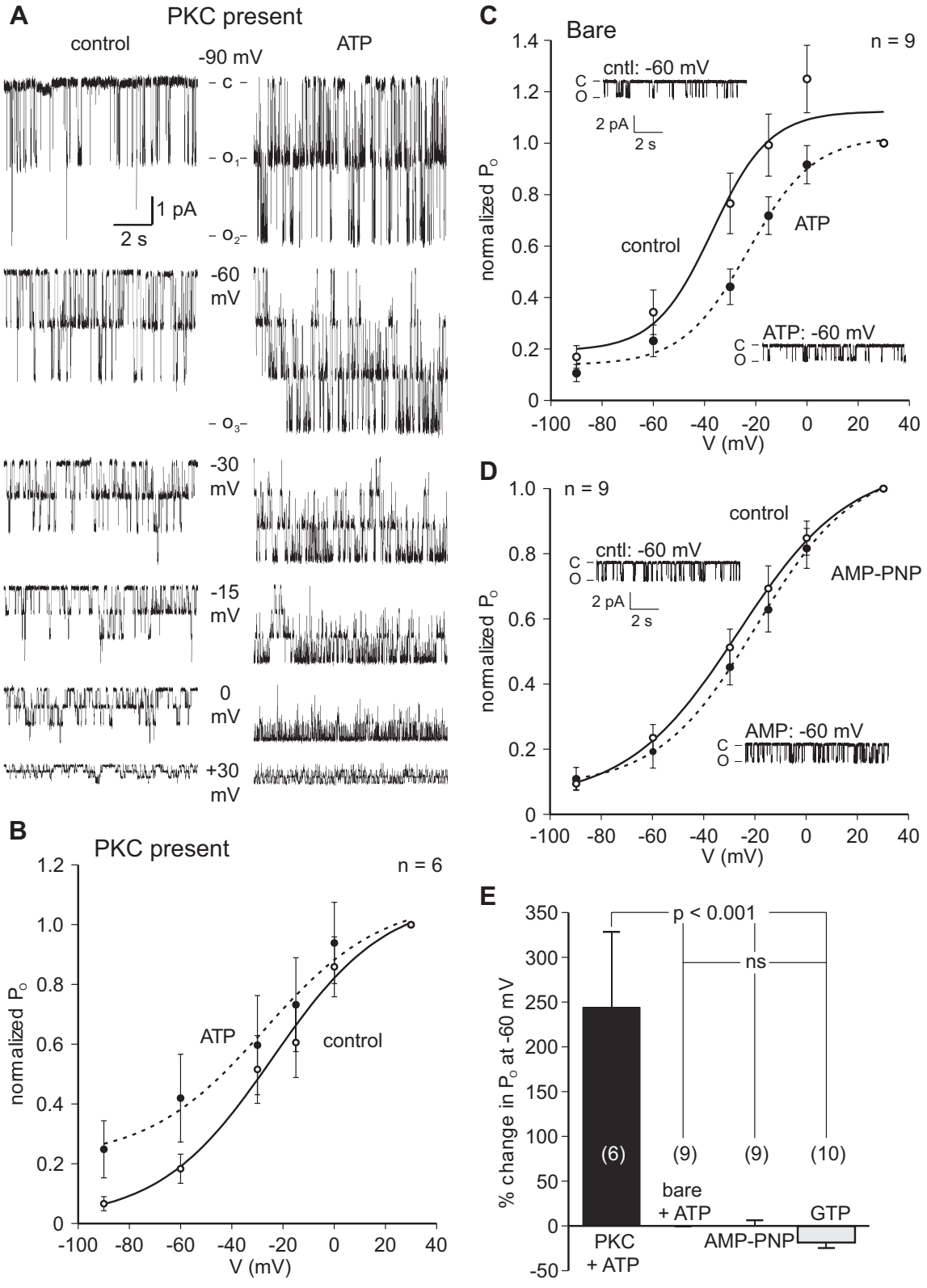

Application of 5 μM IP_3 at -60 mV in 30 μM Ca^{2+}, without any PKC-dependent phosphorylation, had no effect on cation channel activity, with only a $-3 \pm 14\%$ decrease in P_o (Fig. 6*Ai*; $n = 6$). Ca^{2+} dependence was still evident following IP_3 ($n = 6$; Fig. 6*Aii*), although the P_o versus Ca^{2+} concentration curves showed that activity was clearly reduced at every concentration compared with separate control patches ($n = 5$) not exposed to IP_3 (Fig. 6*C*). With application of 1 mM ATP to channels excised into 30 μM Ca^{2+} plus 5 μM IP_3 at -60 mV, there was a $160 \pm 43\%$ increase in P_o, characteristic of phosphorylation by PKC (Fig. 6*Bi*; $n = 7$). After the PKC-induced P_o increase, the Ca^{2+} dependence of these channels in the continued presence of IP_3 and ATP appeared normal (Fig. 6*Bii*) and yielded a P_o versus Ca^{2+} concentration curve ($n = 7$) similar to that of control patches (Fig. 6*C*). Normalization of the three data sets to the activity at 300 μM Ca^{2+} (Fig. 6*D*) provided an EC_{50} of 3 μM for control channels, which was strikingly shifted to the right by IP_3, with an apparent EC_{50} of $\sim$20 M Ca^{2+} (the shift is so dramatic that the fit of the IP_3 curve should be interpreted judiciously). In other IP_3-exposed channels, following phosphorylation and an increased P_o ATP response, the shift in Ca^{2+} dependence was largely restored and the EC_{50} returned to 20 μM.

DISCUSSION

The bag cell neuron afterdischarge is a significant change in excitability and activity that initiates reproduction. Transient synaptic input causes depolarization, fast and slow phases of spiking, and the neural-hemal secretion of egg-laying hormone (Arch 1972; Kaczmarek et al. 1982; Kupfermann 1967, 1970; Kupfermann and Kandel 1970; Loechner et al. 1990; Michel and Wayne 2002; Rothman et al. 1983). At the end of the afterdischarge, the neurons become refractory and respond to further stimuli with only single spikes (Kaczmarek et al. 1978). Many neurons display afterdischarge-like phenomena and/or prolonged depolarizations in the absence of tonic synaptic input, including those involved in motor pattern generation, endocrine control, information storage, and cognition (Andrew and Dudek 1983; Dembrow et al. 2004; Egorov et al. 2002; Haj-Dahmane and Andrade 1997; Russell and Hartline 1982).

Modulation of the cation channel underlying the bag cell neuron afterdischarge likely contributes to the distinct patterns and durations of firing (Wilson and Kaczmarek 1993; Wilson et al. 1996). Triggering the cation channel at the whole cell level is accompanied by release of Ca^{2+} from intracellular stores and translocation of the Ca^{2+}-dependent isoform of PKC to the plasma membrane. (Kachoei et al. 2006; Magoski et al. 2000). Moreover, the depolarization associated with cation channel activation can in part be prevented by inhibition of PKC (Kachoei et al. 2006). The afterdischarge is associated with an upregulation of PKC and an elevation of IP_3 (Fink et al. 1988; Wayne et al. 1999). Our single-channel evidence indicates that IP_3 downregulates the cation channel, dramatically right-shifting Ca^{2+} dependence, whereas PKC has mixed effects, upregulating activity and shifting voltage dependence to the left but Ca^{2+} dependence to the right.

The bag cell neuron cation channel is voltage dependent and noninactivating (Lupinsky and Magoski 2006; Magoski 2004; Wilson et al. 1996). The P_o/V relationship indicates relatively little channel activity at resting membrane potential (-60 mV). However, depolarization during the afterdischarge to between -40 and -20 mV would markedly increase P_o, given that this voltage range is near $V_{1/2}$. In general, changes in membrane potential are translated into different conformational stabilities by the channel voltage sensor (Armstrong and Hille 1998). These changes in channel phenotype correlate with either the duration or number of exponentials required to best fit the kinetic profile of channel dwell times (Colquhoun and Sigworth 1995). We now show that depolarization of the bag cell neuron cation channel decreases the duration of the longest closed time, τ_{C3}, which suggests that the channel favors reopening. Correspondingly, the duration of the longer open time, τ_{O2}, increases with depolarization, signifying the channel also prefers remaining open. This is consistent with the requirements of a steady-state current that maintains the membrane potential at or above the threshold for spiking.

Prior work indicated that PKC directly gates the cation channel because phosphorylation causes a large elevation in P_o (Magoski and Kaczmarek 2005; Magoski et al. 2002; Wilson et al. 1998). The present study showed that, following the PKC-induced P_o increase, cation channel voltage dependence is enhanced with a modest shift in $V_{1/2}$ to the left. However, this does not adequately capture the effect, because the shift is clearly more evident at negative voltages (-30 to -90). In this range, voltage-dependent recruitment of the channel would be greater and provide more depolarizing drive during the afterdischarge. Changes to voltage dependence following PKC-dependent phosphorylation are not uncommon, such as the enhancement of the *Aplysia Slo* K^+ channel during the refractory period (Zhang et al. 2002) and shifting the voltage dependence of *Hermissenda* K^+ channels to the right (Farley and Auerbach 1986). Although there are a few accounts of kinase-mediated regulation of cation channels (Hisatsune et al. 2004; Shi et al. 2004), to our knowledge, this is the first report of cation channel voltage dependence being modulated following phosphorylation. Nevertheless, these upregulatory effects necessitate a means to prevent a feed-forward loop that could pathologically depolarize the cell or promote chronic bursting.

Our observation that the $V_{1/2}$ of bare cation channels is shifted to the right by ATP was unexpected. Prior assays for the effects of phosphorylation were conducted at -60 mV, where bare channels showed no change in P_o with ATP

FIG. 5. PKC-dependent phosphorylation shifts cation channel Ca^{2+} dependence to the right. *A*: excised, inside-out patch held at -60 mV, but in the absence of ATP, and exposed to different cytoplasmic face Ca^{2+} concentrations as indicated. This patch contains 3 cation channels. Channel activity increases with increasing Ca^{2+}. *B*: exposing a different patch to the same Ca^{2+} concentration, but with channels in the phosphorylated state (1 mM ATP, channel-associated PKC). The Ca^{2+}-dependent increase in P_o is again apparent, although as is typical of PKC-phosphorylated channels, the P_o is greater at all concentrations. This patch contains 5 cation channels. *C*: compared with control (●), channels that have undergone phosphorylation (○) show an increase in P_o at every Ca^{2+} concentration. *Inset*: for the PKC-phosphorylated channels, each patch is first held at -60 mV in 30 μM Ca^{2+}, and the cytoplasmic face exposed to ATP. The channel is exposed to different Ca^{2+} concentrations, as per *B*. This patch has 2 cation channels, and P_o increases in the presence of ATP. *D*: the Ca^{2+} dependence of the channel is shifted to the right following the actions of PKC, with a change in EC_{50} from 5.1 to 30.0 μM and a small change in the Hill coefficient from 0.89 to 0.77.

(Magoski and Kaczmarek 2005). That AMP-PNP recapitulates the effect of ATP suggests the shift to the right may be attributed to adenine nucleotide binding, as seen in K^+ and some other cation channels (Bhattacharjee et al. 2003; Chen and Simard 2001; Cho et al. 2003; Csanády and Adam-Vizi 2003; Nilius et al. 2005; Van den Abbeele et al. 1994; Yang et al. 2007). However, because the change in $V_{1/2}$ of bare channels caused by AMP-PNP was less than that of ATP, it is possible that another, as yet unidentified, kinase associates with the channel and contributes to the shift to the right. Because

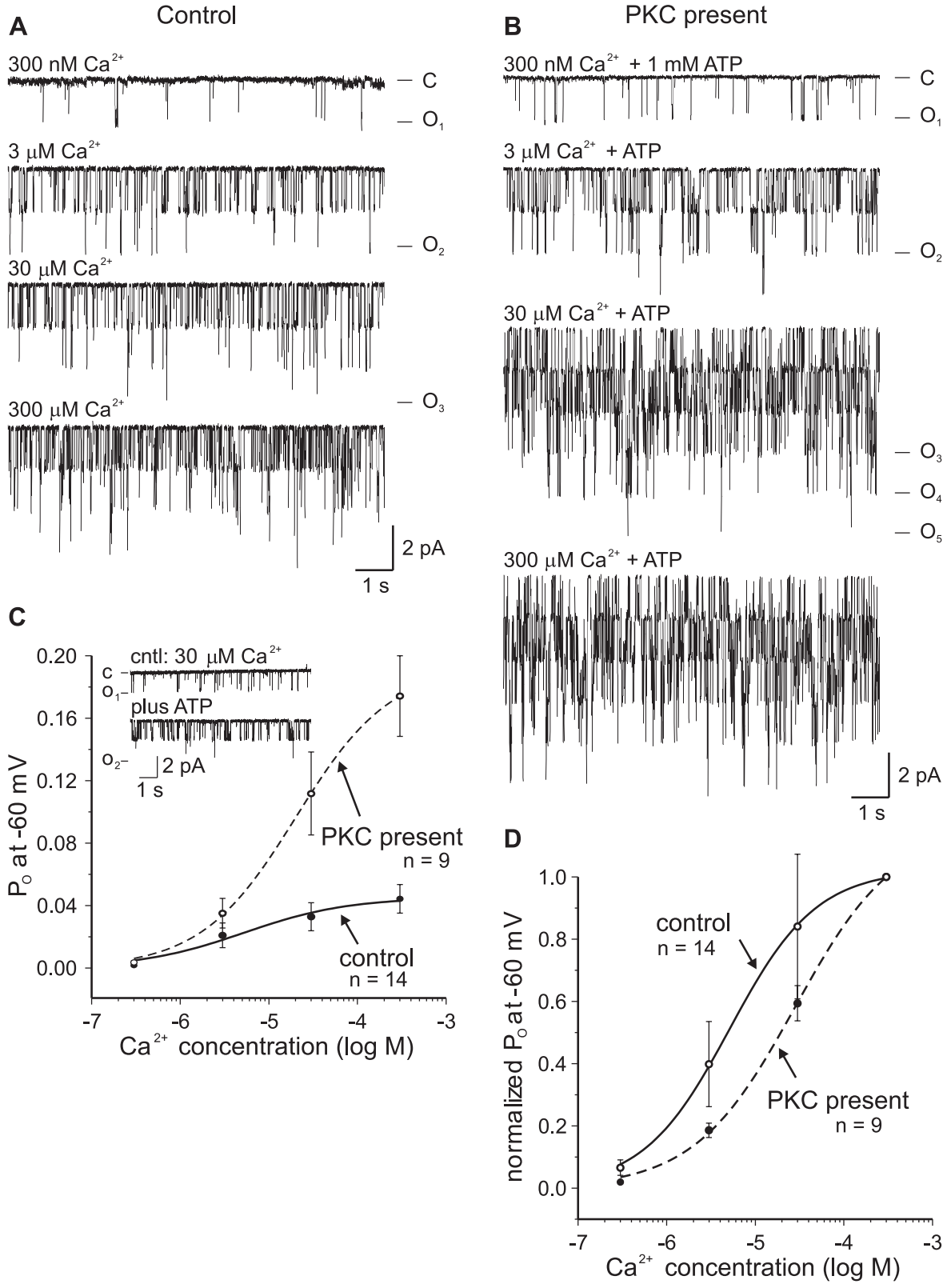

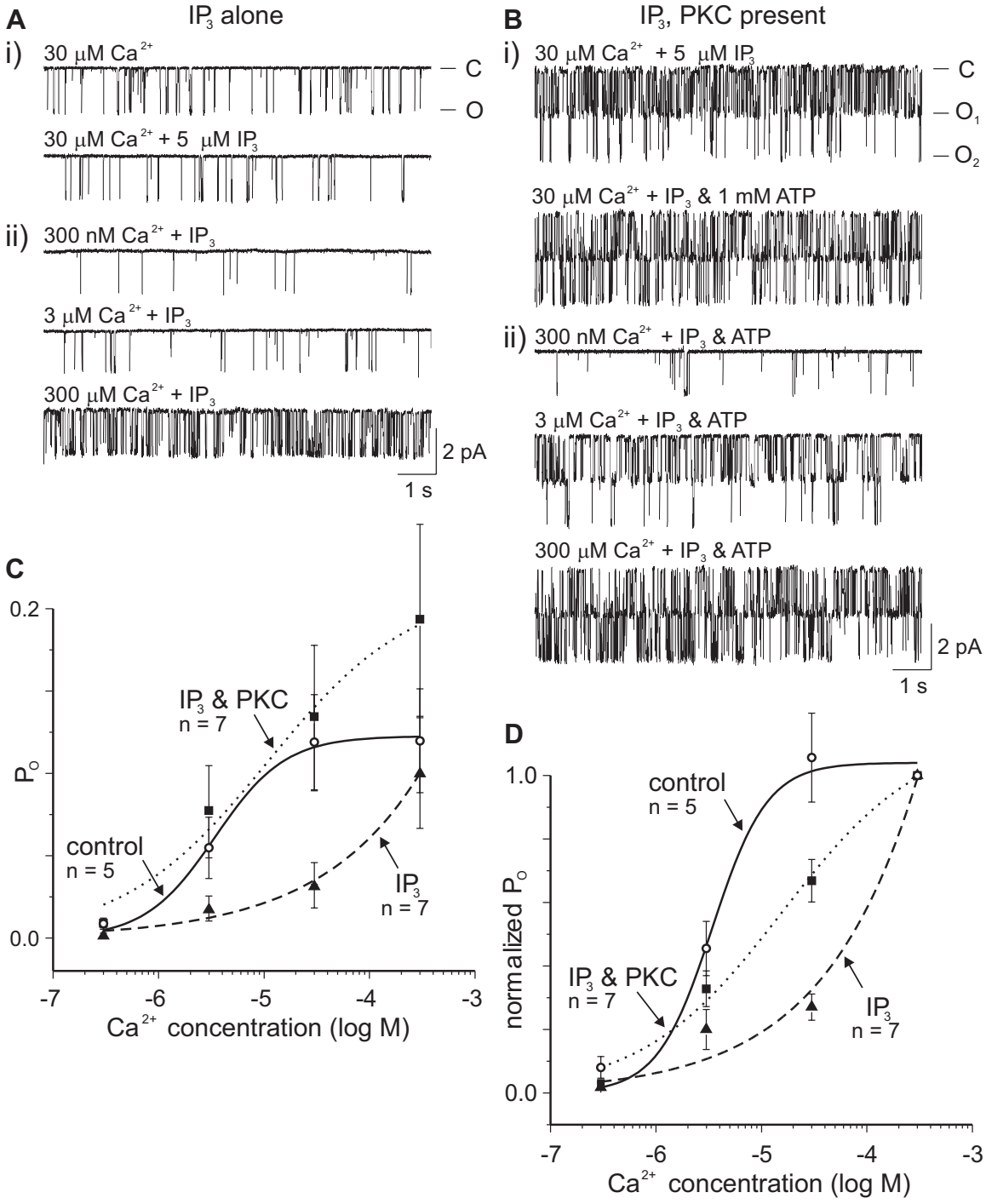

FIG. 6. Inositol trisphosphate (IP_3) shifts cation channel Ca^{2+} dependence to the right, and this is largely negated by PKC. *Ai*: voltage-clamp recordings of an excised, inside-out patch at −60 mV in intracellular solution containing 30 μM Ca^{2+} but no ATP. Application of 5 μM IP_3 to the cytoplasmic face of the patch has no effect on P_o. *Aii*: exposing the same patch to varying Ca^{2+} concentrations along with 5 μM IP_3 shows that Ca^{2+} dependence is still apparent, although not as obvious (cf. Fig. 5*A*). *Bi*: in a different patch, containing 2 channels exposed to 30 μM Ca^{2+} and 5 μM IP_3, addition of 1 mM ATP increases P_o, consistent with PKC-dependent phosphorylation. *Bii*: the same patch, exposed to varying Ca^{2+} concentrations along with 5 μM IP_3 and 1 mM ATP, shows a more typical Ca^{2+} dependence (similar to Fig. 5*B*). *C*: in contrast to control (○), channels treated with just IP_3 (▲) show a decreased P_o at all but the highest Ca^{2+} concentration. For channels that have undergone phosphorylation subsequent to delivery of IP_3 (■), the activity is similar to that shown by control channels. *D*: the Ca^{2+} dependence of cation channel P_o is strongly shifted to the right by IP_3 alone (▲; apparent EC_{50} = 20 M, Hill = 0.49) compared with control (○; EC_{50} = 3.4 μM, Hill = 1.67). However, phosphorylation of the channel in the presence of IP_3 results in recovery of the curve toward control (■; EC_{50} = 20.0 μM, Hill = 0.65).

ATP is omnipresent, the right shift in bare channels is likely more representative of voltage dependence under physiological conditions, and PKC acts on this state.

Like many cation channels, the bag cell neuron channel is Ca^{2+} dependent. We found an EC_{50} of 3–5 μM for Ca^{2+} activation, which is similar to both what our laboratory has

previously published (Lupinsky and Magoski 2006), as well as that reported for other cation channels (Cho et al. 2003; Liman 2003; Liu and Liman 2003; Nilius et al. 2005; Van den Abbeele et al. 1994). The most likely source of Ca^{2+} would be voltage-gated Ca^{2+} channels, where high concentrations can be achieved in microdomains during spiking (Fisher et al. 1994; Geiger and Magoski 2008; Knox et al. 1992; Llinas et al. 1992; Woolum and Strumwasser 1988). Bag cell neuron cation channel Ca^{2+} dependence is shifted to the right following the PKC-induced P_o increase. Because PKC strongly stimulates activity, the P_o is high at all Ca^{2+} concentrations despite the drop in Ca^{2+} responsiveness, which is apparent only when the data are normaliz. This downregulatory aspect may prevent overstimulation of the channel in the face of upregulated voltage dependence and activity. Although kinase-mediated regulation of Ca^{2+} dependence is common (Reinhart et al. 1991), the lone examples we have found for cation channels are a shift to the left of the calmodulin-mediated Ca^{2+} dependence of TRPM4 by PKC (Nilius et al. 2005) and protein kinase A essentially eliminating Ca^{2+} activation in sensory neurons (Razani-Boroujerdi and Partridge 1993).

This study showed that IP_3 strongly shifts bag cell neuron cation channel Ca^{2+} dependence to the right. The channel may have an IP_3 binding site that influences Ca^{2+} calmodulin transduction. IP_3 opens lobster neuron cation channels (Fadool and Ache 1992) and directly potentiates a receptor-operated cation channel in myocytes (Albert and Large 2003). However, *Drosophila* TRPs and vertebrate TRPC channels have a domain that binds calmodulin and the IP_3 receptor (Tang et al. 2001). The IP_3 receptor can even abate the effects of calmodulin by competing for the binding site (Zhang et al. 2001). Furthermore, Kiselyov et al. (1998) suggested that the interaction between TRPC3 and the IP_3 receptor could persist in excised, inside-out patches. Thus it is possible that IP_3 shifts Ca^{2+} dependence by displacing calmodulin in some capacity. The effect of IP_3 on Ca^{2+} dependence is enigmatic: the shift is profound with only IP_3, but the outcome of IP_3 followed by PKC is similar to that of PKC alone. The rescue of Ca^{2+} dependence following the PKC response implies an attenuation, but not an elimination, of IP_3 effectiveness, perhaps by restricting the direct binding of IP_3 or the binding of some IP_3 receptor. This is supported by the absolute P_o versus Ca^{2+} concentration data showing that the ability of PKC to enhance activity at any given concentration is not as effective in the presence of IP_3.

A model for modulation of the bag cell neuron cation channel is shown in Fig. 7. PKC is activated throughout the afterdischarge (Wayne et al. 1999), and although the kinetics of bag cell neuron IP_3 elevation are poorly defined (Fink et al. 1988), evidence from cell lines suggest IP_3 would initially peak and then plateau (Bartlett et al. 2005). Hence, during the fast phase, Ca^{2+}, PKC, and IP_3 levels are likely all high. The channel would be stimulated by depolarization, along with Ca^{2+} and PKC, but this would be kept in check by the inhibitory effects of IP_3 and PKC on Ca^{2+} dependence. During the slow phase, Ca^{2+} levels fall somewhat (Geiger and Magoski 2008; Michel and Wayne 2002), which is probably the case for IP_3 as well. Depolarization is maintained by the upregulatory effect of PKC on activity and voltage dependence. The action of PKC, and to a lesser extent IP_3, on Ca^{2+} dependence would simultaneously restrain activity. The latter may also prime the transition to the refractory period by working in concert with a reorganization of the cation channel modulatory complex. Prior studies show that refractoriness is linked to a decrease in the frequency of the channel–PKC association (Magoski and Kaczmarek 2005).

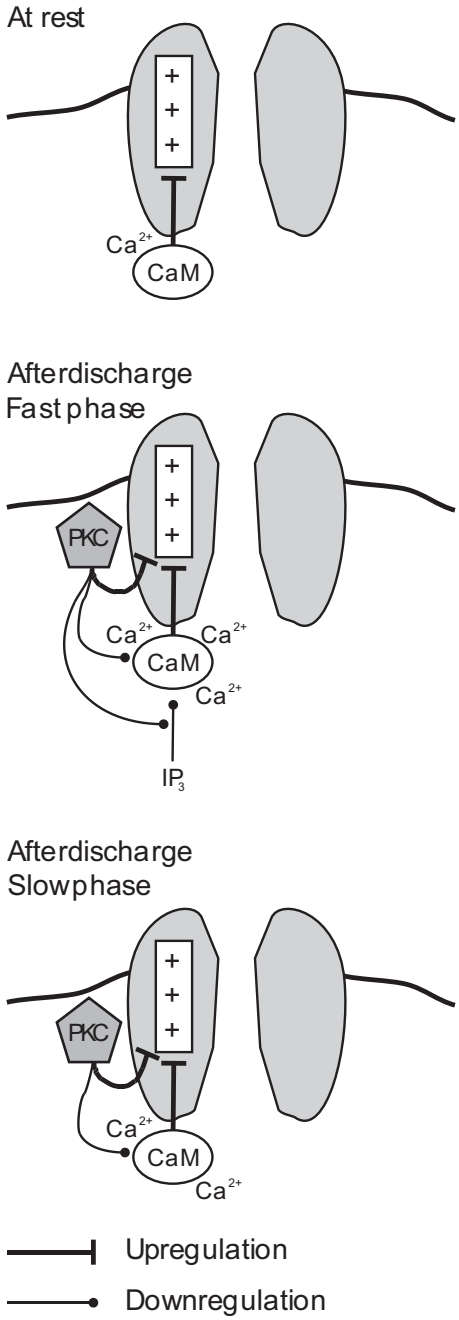

FIG. 7. Multifaceted regulation of the bag cell neuron cation channel. *Top*: at rest, the cation channel is modulated only by closely associated calmodulin (CaM) and low levels of Ca^{2+}. *Middle*: during the fast phase of the afterdischarge, Ca^{2+} levels are very high, and CaM increases channel activity. IP_3 is produced during the afterdischarge, and it dramatically shifts Ca^{2+} dependence to the right. PKC is also associated with the channel during the afterdischarge and upregulates the channel through increased activity, shifting voltage dependence to the left, and disinhibition of IP_3 on Ca^{2+} dependence. PKC plays a downregulatory role by shifting Ca^{2+} dependence to the right. *Bottom*: during the slow phase of the afterdischarge, Ca^{2+} and IP_3 levels both decrease to a plateau. CaM and PKC still exert their modulatory effects. Based on this study as well as Wilson et al. (1996), Magoski et al. (2002), Magoski (2004), Magoski and Kaczmarek (2005), and Lupinsky and Magoski (2006).

In retrospect, the finding that cation channel modulators have opposite effects is not surprising. At the onset of the afterdischarge, depolarization, Ca^{2+} influx, and PKC activation all occur, but if each were upregulatory, spiking may never end. A multifaceted control system provides the potential to achieve a diversity of firing frequencies and release reproductive peptide in the absence of ongoing synaptic input. Furthermore, this may preclude chronic firing and/or behavioral disruption. Similar challenges are likely faced by other neurons that burst or discharge for prolonged periods (Egorov et al. 2002; Fraser et al. 2001; Haj-Dahmane and Andrade 1997; Russell and Hartline 1982). Precise governance over firing frequency is particularly important in cells that secrete peptides or gate sensory information, where subtle changes in rate or pattern can drastically alter output (Hall and Delaney 2002; Morisset and Nagy 1999; Soldo et al. 2004; Vilim et al. 2000). Modulation of the bag cell neuron cation channel could be indicative of how neurons generate but also limit long-term changes in activity.

ACKNOWLEDGMENTS

The authors thank S. L. Smith for technical assistance, N. M. Magoski for evaluation of previous drafts of the manuscript, and two anonymous reviewers for constructive criticism of the work.

GRANTS

K. E. Gardam held an RS McLaughlin Fellowship, and N. S. Magoski holds a Canadian Institutes of Health Research (CIHR) New Investigator Award. This work was supported by a CIHR operating grant to N. S. Magoski.

REFERENCES

Albert AP, Large WA. Synergism between inositol phosphates and diacylglycerol on native TRPC6-like channels in rabbit portal vein myocytes. *J Physiol* 552: 789–795, 2003.

Andrew RD, Dudek FE. Burst discharge in mammalian neuroendocrine cells involves and intrinsic regenerative mechanism. *Science* 221: 1050–1052, 1983.

Arch S. Polypeptide secretion from the isolated parietovisceral ganglion of *Aplysia californica. J Gen Physiol* 59: 47–59, 1972.

Armstrong CM, Hille B. Voltage-gated ion channels and electrical excitability. *Neuron* 20: 371–380, 1998.

Bartlett PJ, Young KW, Nahorski SR, Challiss RAJ. Single cell analysis and temporal profiling of agonist-mediated inositol 1,4,5-trisphosphate, Ca^{2+}, diacylglycerol, and protein kinase C signaling using fluorescent biosensors. *J Biol Chem* 280: 21837–21846, 2005.

Beurrier C, Congar P, Bioulac B, Hammond C. Subthalamic nucleus neurons switch from single-spike activity to burst-firing mode. *J Neurosci* 19: 599–609, 1999.

Bhattacharjee A, Joiner WJ, Wu M, Yang Y, Sigworth FJ, Kaczmarek LK. Slick (Slo2.1), a rapidly-gating sodium-activated potassium channel inhibited by ATP. *J Neurosci* 23: 11681–11691, 2003.

Bicknell RJ, Leng G. Relative efficiency of neural firing patterns for vasopressin release in vitro. *Neuroendocrinology* 33: 295–299, 1981.

Chen M, Simard JM. Cell swelling and a nonselective cation channel regulated by internal Ca^{2+} and ATP in native reactive astrocytes from adult rat brain. *J Neurosci* 21: 6512–6521, 2001.

Cho H, Kim MS, Shim WS, Yang YD, Koo J, Oh U. Calcium-activated cationic channel in rat sensory neurons. *Eur J Neurosci* 17: 2630–2638, 2003.

Colquhoun D, Sigworth FJ. Fitting and statistical analysis of single-channel records. In: *Single Channel Recording* (2nd ed.), edited by Sakmann B, Neher E. New York: Plenum, 1995, p. 483–587.

Conn PJ, Kaczmarek LK. The bag cell neurons of *Aplysia. Mol Neurobiol* 3: 237–273, 1989.

Csanády L, Adam-Vizi V. Ca^{2+}- and voltage-dependent gating of Ca^{2+}- and ATP-sensitive cationic channels in brain capillary endothelium. *Biophys J* 85: 313–327, 2003.

Dembrow NC, Jing J, Brezina V, Weiss KR. A specific synaptic pathway activates a conditional plateau potential underlying protraction phase in the *Aplysia* feeding central pattern generator. *J Neurosci* 24: 5230–5238, 2004.

DeRiemer SA, Schweitzer B, Kaczmarek LK. Inhibitors of calcium-dependent enzymes prevent the onset of afterdischarge in the peptidergic bag cell neurons of *Aplysia. Brain Res* 340: 175–180, 1985.

Egorov AV, Hamam BN, Fransen E, Hasselmo ME, Alonso AA. Graded persistent activity in entorhinal cortex neurons. *Nature* 420: 173–178, 2002.

Fadool DA, Ache BW. Plasma membrane inositol 1,4,5-triphosphate-activated channels mediated signal transduction in lobster olfactory receptor neurons. *Neuron* 9: 907–918, 1992.

Farley J, Auerbach S. Protein kinase C activation induces conductance changes in *Hermissenda* photoreceptors like those seen in associative learning. *Nature* 319: 220–223, 1986.

Fink LA, Connor JA, Kaczmarek LK. Inositol triphosphate releases intracellularly stored calcium and modulates ion channels in molluscan neurons. *J Neurosci* 8: 2544–2555, 1988.

Fisher T, Levy S, Kaczmarek LK. Transient changes in intracellular calcium associated with a prolonged increase in excitability in neurons of *Aplysia californica. J Neurophysiol* 71: 1254–1257, 1994.

Fraser DD, Doll D, MacVicar BA. Serine/threonine protein phosphatases and synaptic inhibition regulate the expression of cholinergic-dependent plateau potentials. *J Neurophysiol* 85: 1197–1205, 2001.

Geiger JE, Magoski NS. Ca^{2+}-induced Ca^{2+} release in *Aplysia* bag cell neurons requires interaction between mitochondrial and endoplasmic reticulum stores. *J Neurophysiol* 100: 24–37, 2008.

Haj-Dahmane S, Andrade R. Calcium-activated cation nonselective current contributes to the fast afterdepolarization in rat prefrontal cortex neurons. *J Neurophysiol* 78: 1983–1989, 1997.

Hall BJ, Delaney KR. Contribution of a calcium-activated non-specific conductance to NMDA receptor-mediated synaptic potentials in granule cells of the frog olfactory bulb. *J Physiol* 543: 819–834, 2002.

Hisatsune C, Kuroda Y, Nakamura K, Inoue T, Nakamura T, Michikawa T, Mizutani A, Mikoshiba K. Regulation of TRPC6 channel activity by tyrosine phosphorylation. *J Biol Chem* 279: 18887–18894, 2004.

Hung AY, Magoski NS. Activity-dependent initiation of a prolonged depolarization in *Aplysia* bag cell neurons: role for a cation channel. *J Neurophysiol* 97: 2465–2479, 2007.

Kachoei BA, Lamb S, Magoski NS. Protein kinase C plays a role in the initiation of bursting in *Aplysia* bag cell neurons. *Soc Neurosci Abstr* 32: 813.6, 2006.

Kaczmarek LK, Jennings K, Strumwasser F. Neurotransmitter modulation, phosphodiesterase inhibitor effects, and cyclic AMP correlates of afterdischarge in peptidergic neurites. *Proc Natl Acad Sci USA* 75: 5200–5204, 1978.

Kaczmarek LK, Jennings K, Strumwasser F. An early sodium and a late calcium phase in the afterdischarge of peptide-secreting neurons of *Aplysia. Brain Res* 238: 105–115, 1982.

Kiselyov K, Xu X, Mozhayeva G, Kuo T, Pessah I, Mignery G, Zhu X, Birnbaumer L, Muallem S. Functional interaction between InsP3 receptors and store-operated Htrp3 channels. *Nature* 396: 478–482, 1998.

Knox RJ, Quattrocki EA, Connor JA, Kaczmarek LK. Recruitment of Ca^{2+} channels by protein kinase C during rapid formation of putative neuropeptide release sites in isolated *Aplysia* neurons. *Neuron* 8: 883–889, 1992.

Kononenko NI, Medin I, Dudek FE. Persistent subthreshold voltage-dependent cation single channels in suprachiasmatic nucleus neurons. *Neuroscience* 129: 85–92, 2004.

Kupfermann I. Stimulation of egg laying: possible neuroendocrine function of bag cells of abdominal ganglion of *Aplysia californica. Nature* 216: 814–815, 1967.

Kupfermann I. Stimulation of egg laying by extracts of neuroendocrine cells (bag cells) of abdominal ganglion of *Aplysia. J Neurophysiol* 33: 877–881, 1970.

Kupfermann I, Kandel ER. Electrophysiological properties and functional interconnections of two symmetrical neurosecretory clusters (bag cells) in abdominal ganglion of *Aplysia. J Neurophysiol* 33: 865–876, 1970.

Liman ER. Regulation by voltage and adenine nucleotides of a Ca^{2+}-activated cation channel from hamster vomeronasal sensory neurons. *J Physiol* 548: 777–787, 2003.

Liu CH, Wang T, Postma M, Obukhov AG, Montell C, Hardie RC. In vivo identification and manipulation of the Ca^{2+} selectivity filter in the *Drosophila* transient receptor potential channel. *J Neurosci* 27: 604–615, 2007.

Liu D, Liman ER. Intracellular Ca^{2+} and the phospholipids PIP_2 regulate the taste transduction ion channel TRPM5. *Proc Natl Acad Sci USA* 100: 15160–15165, 2003.

Llinas R, Sugimori M, Silver RB. Microdomains of high calcium concentration in a presynaptic terminal. *Science* 256: 677–679, 1992.

Loechner KJ, Azhderian EM, Dreyer R, Kaczmarek LK. Progressive potentiation of peptide release during a neuronal discharge. *J Neurophysiol* 63: 738–744, 1990.

Lupinsky DA, Magoski NS. Ca^{2+}-dependent regulation of a non-selective cation channel from *Aplysia* bag cell neurones. *J Physiol* 575: 491–506, 2006.

Magoski NS. Regulation of an *Aplysia* bag cell neuron cation channel by closely associated protein kinase A and a protein phosphatase. *J Neurosci* 24: 6833–6841, 2004.

Magoski NS, Kaczmarek LK. Association/dissociation of a channel-kinase complex underlies state-dependent modulation. *J Neurosci* 25: 8037–8047, 2005.

Magoski NS, Knox RJ, Kaczmarek LK. Activation of a Ca^{2+} -permeable cation channel produces a prolonged attenuation of intracellular Ca^{2+} release in *Aplysia* bag cell neurons. *J Physiol* 522: 271–283, 2000.

Magoski NS, Wilson GF, Kaczmarek LK. Protein kinase modulation of a neuronal cation channel requires protein-protein interactions mediated by an Src homology 3 domain. *J Neurosci* 22: 1–9, 2002.

Mercer AR, Kloppenburg P, Hildebrand JG. Plateau potentials in developing antennal-lobe neurons of the moth, *Manduca sexta. J Neurophysiol* 93: 1949–1958, 2005.

Michel S, Wayne NL. Neurohormone secretion persists after post-afterdischarge membrane depolarization and cytosolic calcium elevation in peptidergic neurons in intact nervous tissue. *J Neurosci* 22: 9063–9069, 2002.

Morisset V, Nagy F. Ionic basis for plateau potentials in deep dorsal horn neurons of the rat spinal cord. *J Neurosci* 19: 7309–7316, 1999.

Nilius B, Prenen J, Tang J, Wang C, Owsianik G, Janssens A, Voets T, Zhu MX. Regulation of the Ca^{2+} sensitivity of the nonselective cation channel TRPM4. *J Biol Chem* 280: 6423–6433, 2005.

Obukhov AG, Nowycky MC. A cytosolic residue mediates Mg^{2+} block and regulates inward current amplitude of a transient receptor potential channel. *J Neurosci* 25: 1234–1239, 2005.

Partridge LD, Swandulla D. Calcium-activated non-specific cation channels. *Trends Neurosci* 11: 69–72, 1988.

Penner R. A practical guide to patch clamping. In: *Single Channel Recording* (2nd ed.), edited by Sakmann B, Neher E. New York: Plenum, 1995, p. 3–30.

Razani-Boroujerdi S, Partridge LD. Activation and modulation of calcium-activated non-selective cation channels from embryonic chick sensory neurons. *Brain Res* 623: 195–200, 1993.

Reinhart PH, Chung S, Martin BL, Brautigan DL, Levitan IB. Modulation of calcium-activated potassium channels from rat brain by protein kinase A and phosphatase 2A. *J Neurosci* 11: 1627–1635, 1991.

Rothman BS, Weir G, Dudek FE. Egg-laying hormone: direct action on the ovotestis of *Aplysia. Gen Comp Endocrinol* 52: 134–141, 1983.

Russell DF, Hartline DK. Slow active potentials and bursting motor patterns in pyloric network of the lobster, *Panulirus interruptus. J Neurophysiol* 48: 914–937, 1982.

Shi J, Mori E, Mori Y, Mori M, Li J, Ito Y, Inoue R. Multiple regulation by calcium of murine homologues of transient receptor potential proteins TRPC6 and TRPC7 expressed in HEK293 cells. *J Physiol* 561: 415–432, 2004.

Soldo BI, Giovannucci DR, Stuenkel EL, Moises HC. Ca^{2+} and frequency dependence of exocytosis in isolated somata of magnocellular supraoptic neurones of the rat hypothalamus. *J Physiol* 555: 699–711, 2004.

Strubing C, Krapivinsky G, Krapivinsky L, Clapham DE. TRPC1 and TRPC5 form a novel cation channel in mammalian brain. *Neuron* 29: 645–655, 2001.

Swandulla D, Lux HD. Activation of a nonspecific cation conductance by intracellular Ca^{2+} elevation in bursting pacemaker neurons of *Helix pomatia. J Neurophysiol* 54: 1430–1443, 1985.

Swensen AM, Bean BP. Ionic mechanisms of burst firing in dissociated purkinje neurons. *J Neurosci* 23: 9650–9663, 2003.

Tahvildari B, Alonso AA, Bourque CW. Ionic basis of ON and OFF persistent activity in layer III lateral entorhinal cortical principal neurons. *J Neurophysiol* 99: 2006–2011, 2008.

Tang J, Lin Y, Zhang Z, Tikunova S, Birnbaumer L, Zhu MX. Identification of common binding sites for calmodulin and inositol 1,4,5-trisphosphate receptors on the carboxyl termini of Trp channels. *J Biol Chem* 276: 21303–21310, 2001.

Van den Abbeele T, Tran Ba Huy P, Teulon J. A Ca^{2+}-activated nonselective cation channel in the basolateral membrane of outer hair cells of the guinea-pig cochlea. *Pfluegers* 427: 56–63, 1994.

Vilim FS, Cropper EC, Price DA, Kupfermann I, Weiss KR. Peptide cotransmitter release from motorneuron B16 in *Aplysia californica*: costorage, corelease, and functional implications. *J Neurosci* 20: 2036–2042, 2000.

Wayne NL, Lee W, Kim YJ. Persistent activation of calcium-activated and calcium-independent protein kinase C in response to electrical afterdischarge from peptidergic neurons of *Aplysia. Brain Res* 834: 211–213, 1999.

Wilson GF, Kaczmarek LK. Mode-switching of a voltage-gated cation channel is mediated by a protein kinase A-regulated tyrosine phosphatase. *Nature* 366: 433–438, 1993.

Wilson GF, Magoski NS, Kaczmarek LK. Modulation of a calcium-sensitive nonspecific cation channel by closely associated protein kinase and phosphatase activities. *Proc Natl Acad Sci USA* 95: 10938–10943, 1998.

Wilson GF, Richardson FC, Fisher TE, Olivera BM, Kaczmarek LK. Identification and characterization of a Ca^{2+}-sensitive nonspecific cation channel underlying prolonged repetitive firing in *Aplysia* neurons. *J Neurosci* 16: 3661–3671, 1996.

Woolum JC, Strumwasser F. Calcium changes in isolated peptidergic neurons during activation by a cAMP analog. *Brain Res* 444: 1–9, 1988.

Yang B, Desai R, Kaczmarek LK. Slack and slick K_{Na} channels regulate the accuracy of timing of auditory neurons. *J Neurosci* 27: 2617–2627, 2007.

Yellen G. Single Ca^{2+}-activated nonselective cation channels in neuroblastoma. *Nature* 296: 357–359, 1982.

Yount RG, Ojala D, Babcock D. Interaction of P-N-P and P-C-P analogs of adenosine triphosphate with heavy meromyosin, myosin and actomyosin. *Biochemistry* 10: 2490–2496, 1971.

Zhang Y, Magoski NS, Kaczmarek LK. Prolonged activation of Ca^{2+}-activated K^+ current contributes to the long-lasting refractory period of *Aplysia* bag cell neurons. *J Neurosci* 22: 10134–10141, 2002.

Zhang Z, Tang J, Tikunova S, Johnson JD, Chen Z, Qin N, Dietrich A, Stefani E, Birnbaumer L, Zhu MX. Activation of Trp3 by inositol 1,4,5-trisphosphate receptors through displacement of inhibitory calmodulin from a common binding domain. *Proc Natl Acad Sci USA* 98: 3168–3173, 2001.